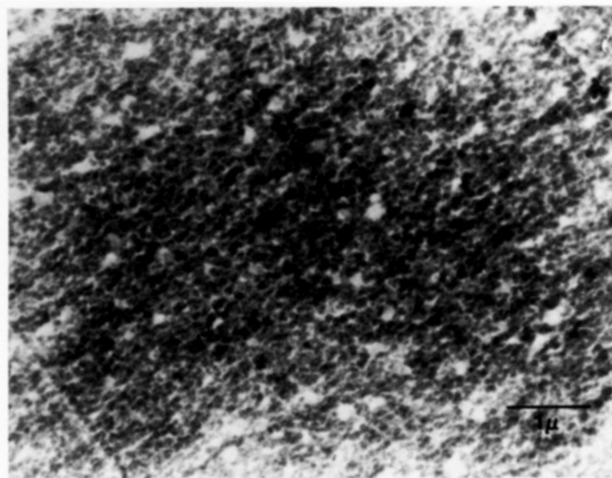

Figure 4. TEM micrograph of a poly[bis(propyl oxybenzoate)phosphazene]/polystyrene IPN.

roughly by NMR integration and also by comparing the heights of the two T_g endotherms. An indication of the significant intermolecular interaction between the constituents is indicated by the (~10 °C) displacement of the T_g's from their original values of −23 (**2**) and 100 °C (**3**).

The homogeneity of the samples was also measured using transmission electron microscopy (TEM). Here, the phase separation of the constituents into individual domains can be seen clearly. The smaller the domain size, the more homogeneous is the sample and the greater the degree of mixing within the sample. Figures 3 and 4 show transmission electron micrographs for IPNs **9** and **11**.

Figure 3 shows a transmission electron micrograph of IPN **9** (MEEP (**1**)/polyacrylonitrile (**5**)). Note the regularity of the small, evenly spaced, almost weblike domain structure. These small domains, along with the single T_g endotherm found in the DSC spectra discussed earlier, show that this is a microheterogeneous, semimiscible system, which could display very different properties from either of its component polymers—MEEP and polyacrylonitrile.

The TEM micrograph of IPN **11** POBP (**2**)/polystyrene (**3**) is shown in Figure 4. This material also possesses a definite domain structure, but the domains are much larger and are well separated, which indicates a less homogeneous structure. This low degree of homogeneity is reflected by the DSC spectra from IPN **11**, which showed two distinct T_g endotherms close to the values for the component polymers. This material should possess properties that are hybrids of the component polymers.

Conclusions. IPNs **7**–**14** represent the first well-characterized interpenetrating polymer networks based on a phosphazene polymer system. The physical properties of these IPNs range from soft and pliable materials to hard and brittle substances, depending on the nature of the component macromolecules. Possible uses for these materials are being studied, especially in biomedical technology.

Acknowledgment. Support for this work from the Office of Naval Research and the National Institutes of Health is gratefully acknowledged.

Registry No. **4**, 9003-53-6; **5**, 9011-14-7; **6**, 25014-41-9; PAA, 9003-01-4.

Pulsed Laser-Assisted Chemical Vapor Deposition of W, Mo, and V Thin Films

W. Turney, Y. M. Hung, S. G. Starcevich, P. S. Cardinahl, and V. H. Grassian*

Department of Chemistry, University of Iowa, Iowa City, Iowa 52242

K. A. Singmaster

Department of Chemistry, San Jose State University, San Jose, California 95192

Received March 26, 1992. Revised Manuscript Received September 21, 1992

A pulsed laser is used to deposit W, Mo, and V films on SiO_2/Si(100) surfaces, from the corresponding metal hexacarbonyl precursor, at two wavelengths, 562 and 281 nm. Film compositions and sputter depth profiles are analyzed with a scanning Auger microprobe. In general, films are contaminated with carbon and oxygen impurities. Film surfaces contain a greater amount of impurities than the bulk of the films. This is most likely due to surface reactions with unreacted hexacarbonyl, following irradiation, and atmospheric gases, during transfer to the analysis chamber. The bulk compositions of W and Mo films are, on average, 65–81% metal, 8–13% carbon, and 10–22% oxygen. An even greater amount of carbon and oxygen is incorporated in the V films at both wavelengths. The results presented here for pulsed laser deposition are compared to previous continuous laser deposition studies.

Introduction

There has been much interest in recent years in the deposition of thin metallic films by laser-assisted chemical vapor deposition (LCVD) because of its important applications in microelectronics device fabrication.[1] In LCVD, a substrate held in a chamber with the vapor of the organometallic precursor is laser irradiated. The organometallic decomposes, and a metal film is deposited on the substrate. One group of precursors that has received a great deal of attention is the metal carbonyls.

Cr, Mo, W, Fe, and Ni films have been produced from the corresponding carbonyl with both continuous-wave (CW)[2-8] and pulsed[2,9-17] laser sources. Carbonyl precursors

* To whom correspondence should be addressed.

(1) *Laser Microfabrication, Thin film Processes and Lithography*; Erlich, D. J., Tsao, J. Y., Eds.; Academic Press: New York, 1989.
(2) Herman, I. P. *Chem. Rev.* **1989**, *89*, 1323 and references therein.

0897-4756/92/2804-1192$03.00/0 © 1992 American Chemical Society

offer several advantages. They exhibit appreciable vapor pressures, possess high photochemical quantum yields in the UV, and are commercially available. However, films deposited by laser irradiation of carbonyl precursors are typically contaminated with high levels of carbon and oxygen.[2-17] Studies in this area have been directed toward understanding the complex chemistry that occurs during laser deposition, in order to develop methods for removing impurities.

Recently, CW laser sources have been used to elucidate deposition mechanisms for Cr, Mo, and W films from hexacarbonyl precursors.[3,4,20] Photochemical deposition in the absence of substrate heating can be accomplished with a CW-UV laser source (e.g., frequency doubled Ar^+ laser at 257 nm).[3] Films deposited in this manner are found to be quite impure (only 20–50% metal). Several sources contribute to the high impurity levels in the films. The presence of oxygen-containing background gases in the reaction chamber during deposition as well as exposure of films to air after deposition have been shown to increase the level of impurities.[3,18] Incomplete decarbonylation of the precursor and adsorption of background CO produced during deposition can also play a role.[19]

Much cleaner films of Cr, Mo and W (80–100% metal) can be produced with CW-visible irradiation (e.g., Ar^+ laser at 514 nm).[4] Under these conditions, the deposition mechanism is primarily thermal in nature due to laser heating of the substrate and growing film. Calculations of the temperature profile of the substrate indicate that for temperatures above 450 K, CO is completely removed from the growing film.[20] However, for $T < 450$ K the dissociation of CO does compete favorably with desorption allowing for carbon and oxygen impurities to be incorporated in the growing film.

Pulsed laser deposition studies can provide additional mechanistic information regarding the deposition process. A pulsed UV laser with its high peak powers typically combines both photochemical (single and multiphoton processes) and thermal deposition mechanisms.[2] The addition of a thermal mechanism should enhance the desorption of CO; it may be expected that UV pulsed lasers produce films with lower levels of carbon and oxygen impurities than CW lasers. Studies reported thus far on the deposition of Mo films do not provide clear evidence of this. Radloff et al.[13] report films deposited with excimer laser (248 nm) irradiation contain 38% Mo, 18% C, and 44% O, while Solanki et al.[10] report values around 92% Mo, 1% C, and 7% O. Flynn and co-workers report the presence of C and O in Mo films deposited with an excimer laser (248 nm) but do not specify the amount.[9]

In contrast, pulsed LCVD with visible wavelengths may be expected to produce films with higher impurity levels than CW-irradiated films. For both pulsed and continuous visible irradiation, the deposition mechanism is expected to be predominantly thermal in nature. (Although, it has been shown that multiphoton decomposition of metal carbonyls can be significant down to 600 nm.[21-23]) However, transient heating with a pulsed laser may affect the deposition mechanism due to the spatial and temporal variation in surface temperature as compared to steady-state heating with a CW laser. It is possible that the level of impurities incorporated in the growing film may be greater for films deposited with pulsed visible laser irradiation because of the temperature dependence of the relative rates of CO dissociation and desorption. Literature data to support this hypothesis are unavailable because compositional studies of pulsed visible LCVD from the metal hexacarbonyls have not been previously reported.

In this paper, we report compositional studies of films deposited from $W(CO)_6$ and $Mo(CO)_6$ by irradiation with 562- and 281-nm pulsed laser light. The data presented here will be compared to films deposited with CW laser light at comparable wavelengths. The pulsed laser studies can provide additional insight into the origin of contaminants in LCVD.

We also report the results of pulsed LCVD of vanadium films from $V(CO)_6$. To the best of our knowledge, this is the first time $V(CO)_6$ has been used in LCVD. We are interested in comparing the composition of vanadium films deposited from $V(CO)_6$ to the composition of other metal films, e.g., Cr, Mo, and W, deposited from the corresponding hexacarbonyls. $V(CO)_6$ is a paramagnetic compound with 17 electrons, the only paramagnetic carbonyl complex known,[24] and its electronic structure could render it more reactive than other carbonyl precursors.

Experimental Section

Films are deposited with the laser beam directed perpendicular to the silicon substrate. The second harmonic of a pulsed (7-ns fwhm) Nd:YAG laser (Continuum YG-661), operated at 10 Hz, is used to pump a dye laser (Continuum TDL-60). Rhodamine 590 is used in these experiments to produce both 562-nm light and the UV light at 281 nm, produced by frequency doubling in a KDP crystal. A Pellin Broca prism separates the dye fundamental from the frequency-doubled light.

The substrate, a Si(100) wafer covered with a native SiO_2 layer, is cleaned with methanol and dried with N_2 gas prior to loading in the deposition chamber. The chamber is pumped by a 20 L/s ion pump, and after an overnight bake-out the pressure in the chamber is less than 1×10^{-8} Torr.

The hexacarbonyl precursors are freeze–pumped–thawed several times prior to each experiment and the chamber is subsequently back-filled with the metal hexacarbonyl vapor. Because of its instability, $V(CO)_6$ is kept at 273 K during deposition and is stored in the dark at 277 K when not in use. The vapor pressure

(3) Singmaster, K. A.; Houle, F. A.; Wilson, R. J. *J. Phys. Chem.* 1990, *94*, 6864.
(4) Singmaster, K. A.; Houle, F. A. *Mater. Res. Soc. Symp. Proc.* 1991, *201*, 209.
(5) Gluck, N. S.; Wolga, G. J.; Bartosch, C. E.; Ho, W.; Ying, Z. *J. Appl. Phys.* 1987, *61*, 998.
(6) Ehrlich, D. J.; Osgood, R. M.; Deutsch, T. F. *J. Electrochem. Soc.* 1981, *128*, 2039.
(7) Jackson, R. L.; Tyndall, G. W. *J. Appl. Phys.* 1988, *64*, 2092.
(8) Gilgen, H. H.; Cacouris, T.; Shaw, P. S.; Krchnavek, R. R.; Osgood, R. M. *Appl. Phys. B* 1987, *42*, 55.
(9) Flynn, D. K.; Steinfeild, J. I.; Sethi, D. S. *J. Appl. Phys.* 1986, *59*, 3914.
(10) Solanki, R.; Boyer, P. K.; Collins, G. J. *Appl. Phys. Lett.* 1982, *41*, 1048.
(11) Allen, S. D.; Tringube, A. B. *J. Appl. Phys.* 1983, *54*, 1641.
(12) Jackson, R. L.; Tyndall, G. W.; Sather, S. D. *Appl. Surf. Sci.* 1989, *36*, 119.
(13) Radloff, W.; Hohmann, H.; Ritze, H. H.; Paul, R. *Appl. Phys. B* 1989, *49*, 301.
(14) Mayer, T. M.; Fisanick, G. J.; Eichelberg, T. S. *J. Appl. Phys.* 1982, *53*, 8462.
(15) Konstantinov, L.; Nowak, R.; Hess, P. *Appl. Phys. A* 1988, *47*, 171.
(16) Haigh, J. *Chemtronics* 1986, *1*, 134.
(17) Aylett, M. R. *Chemtronics* 1986, *1*, 146.
(18) Cho, C. C.; Bernasek, S. L. *J. Appl. Phys.* 1989, *65*, 3035.
(19) Flitsch, F. A.; Swanson, J. R.; Friend, C. M. *Surf. Sci.* 1991, *245*, 85.
(20) Houle, F. A.; Singmaster, K. A. *J. Phys. Chem.*, in press.
(21) Fisanick, G. J.; Gedanken, A.; Eichelberger, T. S.; Keubler, N. A.; Robin, M. B. *J. Chem. Phys.* 1981, *75*, 5215.
(22) Duncan, M. A.; Dietz, T. G.; Smalley, R. E. *Chem. Phys.* 1979, *44*, 415.
(23) Gerrity, D. P.; Rothberg, L. J.; Vaida, V. *Chem. Phys. Lett.* 1980, *74*, 1.
(24) Geoffroy, G. L.; Wrighton, M. S. *Organometallic Photochemistry*; Academic Press: New York, 1979.

Table I. Summary of Auger Data: W Films

film	av C/W	av O/W	range C/W	range O/W	% composition C	% composition O	% composition W
562 nm							
unsputtered	0.7	2.8	0.3–1.3	1.5–5.5	20	29	51
sputtered	0.2	0.6	0.1–0.3	0.1–1.1	9	10	81
281 nm							
unsputtered	1.2	4.9	0.7–1.9	3.9–5.5	26	37	37
sputtered	0.3	1.5	0.2–0.3	1.3–1.7	8	21	71
predicted							
WCO	1.8	5.0			33	33	33
WC_2O_2	3.6	10.0			40	40	20

Table II. Summary of Auger Data: Mo Films

film	av C/Mo	av O/Mo	range C/Mo	range O/Mo	% composition C	% composition O	% composition Mo
562 nm							
unsputtered	0.3	0.7	0.2–0.3	0.5–1.2	21	26	53
sputtered	0.07	0.3	0.04–0.1	0.1–0.6	10	15	75
281 nm							
unsputtered	0.4	2.2	0.2–0.6	1.7–2.6	24	46	30
sputtered	0.2	0.5	0.1–0.2	0.4–0.5	13	22	65
predicted							
MoCO	0.5	1.5			33	33	33
MoC_2O_2	1.0	3.0			40	40	20

Table III. Summary of Auger Data: V Films

film	av C/V	av O/V	range C/V	range O/V[a]	% composition C	% composition O	% composition V
562 nm							
unsputtered	0.5	1.8	0.4–0.8	1.5–2.3	33	42	26
sputtered	0.4	0.7	0.3–0.5	0.5–0.9	40	24	36
281 nm							
unsputtered	0.4	2.5	0.3–0.5	2.5–2.6	24	53	23
sputtered	0.5	0.8	0.4–0.5	0.7–0.8	45	22	33
Standards							
V_2O_5							
unsputtered		2.9					
sputtered		2.9 (predicted O/V = 2.8)					
V_2O_3							
unsputtered		2.9					
sputtered		2.0 (predicted O/V = 1.7)					
VC							
unsputtered	0.2						
sputtered	0.8 (predicted C/V = 0.4)						

[a] Vanadium and oxygen have overlapping Auger transitions.

for $V(CO)_6$ is measured to be near 250 mTorr when the sample is held at 273 K. The room-temperature vapor pressures for $W(CO)_6$ and $Mo(CO)_6$ are 19 and 85 mTorr, respectively.

The silicon wafer is kept at room temperature or cooled with liquid nitrogen during deposition. We found it necessary to cool the substrate when depositing at 281 nm so that the concentration of $M(CO)_6$ was greatest at the sample surface; otherwise deposition onto the window was sufficiently heavy to block transmission of the laser light.

The unfocused laser beam (6-mm diameter) is incident on the silicon wafer through either a sapphire viewport for 281-nm deposition or a Pyrex viewport for 562-nm deposition. The number of laser shots ranged from 3000 to 30 000 for each film deposited.

After the film is deposited, the chamber is evacuated with a turbomolecular pump and then back-filled with N_2 gas. The sample is transferred under a nitrogen atmosphere to a scanning Auger microprobe where it is introduced into the ultrahigh-vacuum chamber. The sample is exposed to air for several seconds (5–15 s) during this process. The transfer procedure minimizes oxidation of film surfaces by air but does not completely inhibit the process.

A PHI Model 3067 3μ scanning Auger microprobe is used for Auger electron spectroscopy (AES). The base pressure of the ultrahigh-vacuum chamber is typically 5×10^{-10} Torr. A beam energy of 5 keV and beam current of 20 nA are used to collect Auger data. The ion sputtering gun is operated at 2 keV and sputtering rates of approximately 1.5 Å/s are obtained with this system.

Vanadium standards, VC (technical grade), V_2O_3(99%), and V_2O_5(99.9%), were purchased from Aldrich and used without further purification. V_2O_3, V_2O_5, and VC, as well as the hexacarbonyl precursors, are toxic; necessary precautions should be taken when handling these compounds.

Results

Tables I–III list the elemental compositions and peak-to-peak height ratios for W, Mo, and V films, respectively, deposited at 562 and 281 nm. Also listed in the tables are predicted compositions for several stoichiometries calculated from Auger sensitivities at 5 keV.[25] Peak-to-peak height ratios obtained for vanadium carbide and oxide standards imbedded in In foil are included in Table III. Peak-to-peak height ratios are determined from the following Auger transitions: Mo (MNN, 186 eV), C (KLL, 272 eV), V (LMM, 473 eV), O (KLL, 503 eV), and W (MNN, 1736 eV). Compositions for unsputtered (film surface) and sputtered (film bulk) films are given. Percent compositions are calculated from average peak-to-peak height ratios and are provided for the purpose of comparison to previous studies.

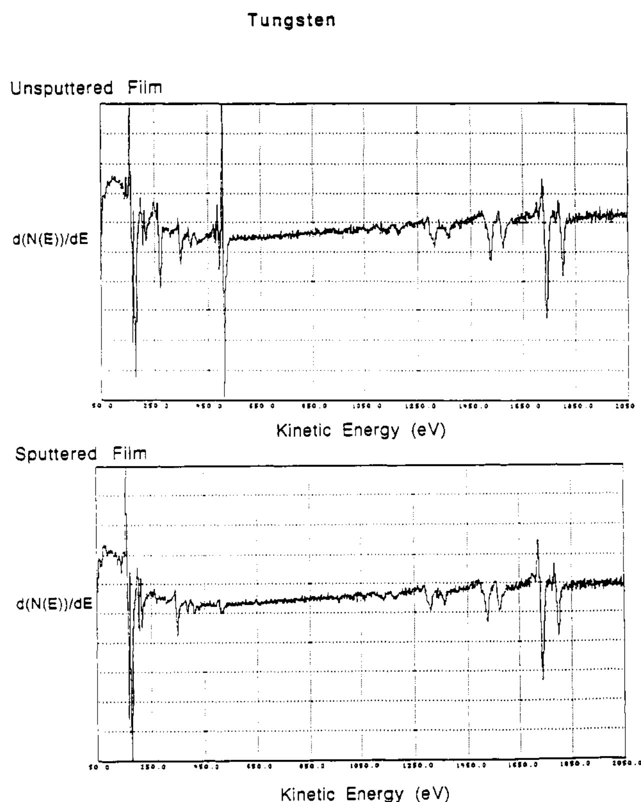

Figure 1. Auger spectra of a W film deposited with 562-nm light using a laser energy of 38 mJ/pulse; unsputtered (film surface) and sputtered (film bulk).

In the presence of the metal hexacarbonyl vapor, irradiation of the substrate at room temperature with an unfocused laser beam at 281 nm did not lead to appreciable film deposition even after prolonged exposure. However, significant levels of deposition were observed on the photolysis cell window. As discussed in the Experimental Section, it was necessary to cool the Si substrate with liquid nitrogen before irradiation. Cooling the sample produced a condensed layer of metal hexacarbonyl on the substrate and reduced the problem of deposition at the window. Because the metal hexacarbonyls are transparent to visible light, irradiation at 562 nm did not require cooling of the substrate. Therefore, depositions with 562-nm light were done with the substrate at room temperature and window deposits, although sometimes present, were not as problematic as they were for UV deposition.

W Films. Figure 1 shows typical Auger spectra of W deposited at 562 nm before and after sputtering. Seven films were deposited with laser energies ranging from 17 to 47 mJ/pulse. As significant compositional differences between the laser energies were not detected, the data present in Table I are averaged for these seven films.

The surface composition of the films (unsputtered) deposited with 562-nm light shows appreciable quantities of carbon and oxygen. Comparison to predicted peak-to-peak height ratios indicates a film surface composition consistent with approximately one CO per two W atoms. It is interesting to note that although films are briefly exposed to air during transfer to the analysis chamber, the amount of oxygen on the film surface is relatively low. The complete formation of stable oxides, such as WO_2 and WO_3, does not occur.

As the sample is sputtered, there is a significant decrease in the C and O levels. This decrease is accomplished in the first 150 Å of sputtering. The film bulk stoichiometry is near the level of one CO per eight W atoms. This decrease is real and does not reflect effects such as preferential sputtering of oxygen.[3] Although the reduction of impurities is significant, there are still detectable amounts of carbon and oxygen throughout the bulk of the film.

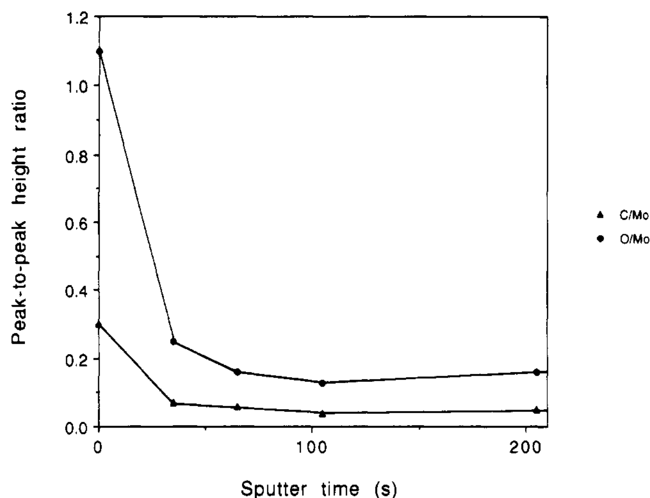

Figure 2. Auger depth profile of a Mo film deposited with 562-nm laser light. The sputter rate is 1.5 Å/s.

The data presented in Table I for W films deposited using 281-nm irradiation, before and after sputtering, represent the results of four different samples deposited with laser energies in the range 14–18 mJ/pulse. The composition of the film surface is in the range of one CO per W atom.

The bulk of the film is cleaner than the surface. The reduction of oxygen levels during sputtering occurred within the first 150 Å, again indicating that preferential sputtering of oxygen was not a problem. Bulk compositions are on the order of one to two CO groups per seven W atoms.

Mo Films. Table II includes data for both 281 and 562 nm irradiation of $Mo(CO)_6$. Films deposited with 562-nm laser light are relatively clean (low C/Mo and O/Mo ratios) and indicate a film surface stoichiometry of one CO per two Mo atoms. The results for five films deposited at 562 nm and laser energies ranging from 26 to 49 mJ/pulse are included in Table II. Due to film deposition on the chamber window, the laser energy incident on the substrate decreased with time. The reported values are the initial laser energies.

Sputtering removes some, but not all, of the carbon and oxygen impurities. In Figure 2 the C/Mo and O/Mo ratios have been plotted as a function of film depth for the first 320 Å. As shown in Figure 2, the O/Mo and C/Mo ratios decrease significantly within the first 100 Å and then remain nearly constant in the bulk of the film. In the bulk, a stoichiometry of one to two CO groups per eight Mo atoms is seen.

Four different films were deposited at 281 nm with laser energies ranging from 2 to 18 mJ/pulse. The results are given in Table II. Line-shape analysis of the carbon peak at 272 eV indicates the presence of graphitic carbon on the surface. Upon sputtering, the carbon and oxygen peaks decrease and line-shape analysis of the carbon peak indicates the presence of carbidic carbon in the bulk of the film.

V Films. $V(CO)_6$ is a dark blue solid while $W(CO)_6$ and $M(CO)_6$ are white powders. To determine the absorption properties of $V(CO)_6$, the UV–vis spectrum of $V(CO)_6$ was recorded in the gas phase at room temperature. In agreement with published literature data, the spectrum consists of two intense features near 260 nm and two

weaker features at 348 and 400 nm.[26,27] The two peaks near 260 nm have been attributed to charge-transfer absorptions, and the weaker features have been assigned to metal-centered d–d transitions.[26,27] Since gas-phase $V(CO)_6$ does not absorb visible light, the origin of the dark color of the solid is not well understood.[24]

Analysis of the Auger spectra for deposited vanadium films is complicated by overlapping Auger transitions between vanadium and oxygen. Vanadium exhibits a strong AES transition at 473 eV, with a weaker transition near 509 eV.[25] Oxygen also exhibits multiple transitions in this region with a strong transition at 503 eV and two weaker ones at 468 and 483 eV.[25] The weaker transitions of both V and O are on the order of 20% the intensity of the stronger transitions. The peaks due to the weaker transitions of either element could perturb the intensity of the peak of the strongest transition associated with the other element.

Analysis of vanadium oxide standards is needed to estimate film stoichiometries. Table III includes peak-to-peak height ratios for two vanadium oxides, V_2O_5 and V_2O_3, and vanadium carbide. Both vanadium oxide powders exhibit an oxygen to vanadium peak-to-peak height ratio of 2.9 at the surface. Sputtering V_2O_3 results in a ratio of 2.0, whereas the ratio for V_2O_5 remains constant after sputtering. The predicted values for the oxides based on AES sensitivities at 5 keV[25] are 1.7 for V_2O_3 and 2.8 for V_2O_5. The predicted values are close to those observed experimentally. Given the appreciable ranges of O/V ratios observed for the films and the good agreement between the experimental and predicted peak-to-peak height ratios for the vanadium oxide standards, the error introduced by ignoring overlapping transitions does not significantly affect the analysis of the films.

The oxide standards also show that preferential sputtering of oxygen is not a problem. The O/V ratio in V_2O_5 undergoes no change during sputtering, and although the oxygen level decreases in V_2O_3, it does not go below the predicted value. The higher oxygen content on the trioxide surface might be attributed to dissolved oxygen; such an effect is observed for Cr_2O_3.[28,29]

The carbide sample exhibits high levels of oxygen on the surface which rapidly decreases, but does not disappear, upon sputtering. The predicted value for the carbon to vanadium peak-to-peak height ratio is 0.4,[25] somewhat less than that experimentally determined value of 0.8 for the carbide standard.

Table III includes data for V films deposited with 562- and 281-nm pulsed laser light. Laser energies range from 18 to 41 and 15 to 17 mJ/pulse for deposition at 562 and 281 nm, respectively. At least two films were deposited at each wavelength. In Figure 3, typical Auger spectra for films deposited at 281 nm, before and after sputtering, are shown. All films exhibit significant levels of carbon and oxygen, even after sputtering for several minutes. Unlike the Mo and W films, the vanadium films exhibit an appreciable oxygen concentration gradient in the first several hundred angstroms (300–400 Å). Figure 4 shows C/V and O/V ratios plotted as a function of sputter time. Analysis of the oxide standards discussed above indicates that preferential sputtering is not a problem. Therefore, the oxygen concentration gradient is real and must reflect the greater reactivity of oxygen with V as compared to Mo and W. The V film surface and bulk have comparable levels of C, unlike Mo and W films where carbon levels decrease significantly in the bulk. The Auger spectra also reveal that carbon on the film surface is graphitic in nature and carbidic in the bulk of the film. Comparison of peak-to-peak height ratios obtained for sputtered films to predicted values and vanadium standards give a stoichiometry of VCO.

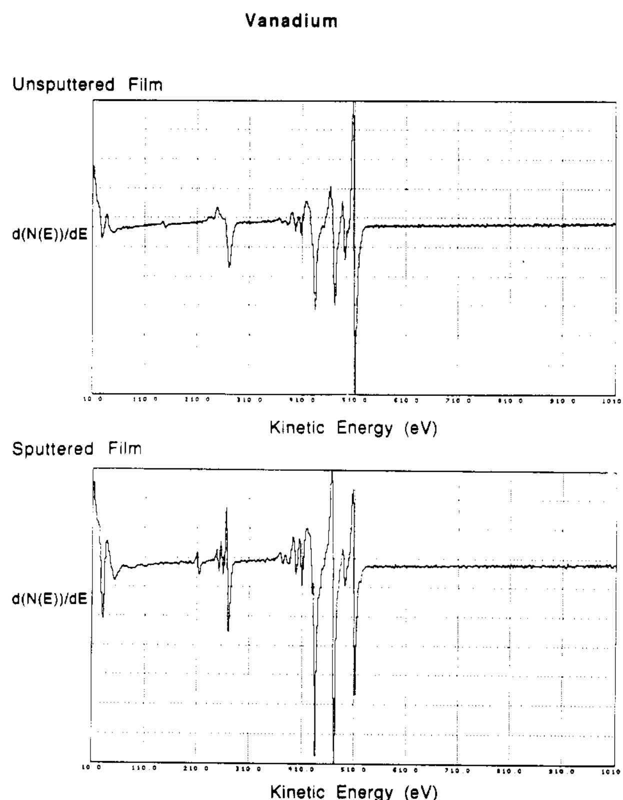

Figure 3. Auger spectra of a V film deposited with 281-nm light using a laser energy of 16 mJ/pulse; unsputtered (film surface) and sputtered (film bulk).

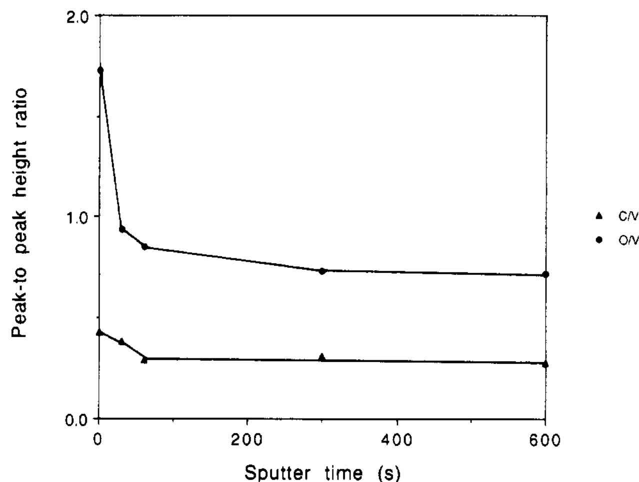

Figure 4. Auger depth profile of a V film deposited with 562-nm laser light. The sputter rate is 1.5 Å/s.

Sources of Error. Although beam damage and preferential sputtering of oxygen are possible sources of error in the Auger analysis, the experimental conditions were chosen to minimize these effects. We did not observe any changes in the Auger data as a function of time for these

(25) Davis, L. E.; MacDonald, N. C.; Palmberg, P. W.; Riach, G. E.; Weber, R. E. *Handbook of Auger Electron Spectroscopy*, 2nd ed.; Perkin-Elmer Corp.: Eden Prairie, MN, 1976.
(26) Hass, H.; Sheline, R. K. *J. Am. Chem. Soc.* **1966**, *88*, 3219.
(27) Rubinson, K. A. *J. Am. Chem. Soc.* **1976**, *98*, 5188.
(28) Dolle, P.; Alnot, M.; Ehrhardt, J. J.; Cassuto, A. *J. Electron Spectrosc. Relat. Phenom.* **1979**, *17*, 299.
(29) Kim, K. S.; Baitinger, W. E.; Amy, J. W.; Winograd, N. *J. Electron Spectrosc. Relat. Phenom.* **1974**, *5*, 531.

films. Therefore, it is expected that all but instantaneous beam damage effects have been eliminated. Preferential sputtering of oxygen is a common problem in W and Mo oxides. The results of preferential sputtering of such standards have been discussed fully in ref 3 and do not constitute a major problem in these studies. The vanadium oxide standards investigated here likewise do not appear to undergo preferential sputtering of oxygen.

Discussion

Effect of Exposure to Air on Inherent Film Stoichiometries for W and Mo Films. Precise information regarding deposition mechanisms and inherent film compositions are best obtained from films deposited under high-vacuum conditions and vacuum-transferred to the analysis chamber. In the pulsed laser studies described here, it was not possible to transfer the films in vacuum. Exposure of films to air prior to analysis can cause changes in the surface and bulk film compositions.[3,4]

In general, film surfaces are found to contain higher levels of carbon and oxygen impurities than the bulk of the films (see Tables I–III). Reactions at the film surface with unreacted parent hexacarbonyl, after laser irradiation, and with atmospheric gases, during transfer to the analysis chamber, are probably the cause of the differences in film surface and bulk compositions. To determine the inherent film composition obtained in pulsed LCVD of W and Mo films from $Mo(CO)_6$ and $W(CO)_6$, the effect of exposure to air on film composition must be understood. A possible way in which to assess the effect of exposure to air on film composition in the present study is to compare with previous results using CW-visible laser irradiation. It was found that the bulk compositions did not differ between films exposed to air and those which were vacuum-transferred, for films deposited with a Ar^+ ion laser. However, compositional changes were observed for the film surfaces and the amount of carbon and oxygen increased when films were exposed to air.[4,20] We can assume that the situation is similar for films deposited with a pulsed visible laser and the bulk composition represents the inherent composition, while the surface composition reflects somewhat higher levels of C and O due to exposure to air. The bulk stoichiometries found for films deposited at 562 nm then are on the order of one CO for every eight metal atoms for both Mo and W films.

Determining the inherent film compositions for UV-deposited films is somewhat more difficult. Electron micrographs of films deposited with a frequency-doubled Ar^+ laser reveal that film ripples exist and that the films are quite porous.[3] The open morphology of the films allows for easy intercalation and subsequent oxidation and is reflected in the composition differences between films exposed to air and films which were vacuum-transferred.[3] The data for films analyzed in ref 3 show that the surface C/M ratio for vacuum-transferred films falls between the ratios obtained for the film surface and bulk when exposed to air. Taking these effects into consideration and assuming a level of oxidation comparable to that of the CW films (a worst case scenario), we estimate the C/M ratios, for pulsed UV deposited films, to be in the ranges 1.2–0.3 and 0.4–0.2 for W and Mo, respectively, after sputtering. Bulk oxygen levels are, at worse, those observed after sputtering. The bulk stoichiometries of both W and Mo films are approximately one CO per three metal atoms.

Pulsed Visible LCVD of Mo and W Films. Pulsed LCVD of Mo and W films from hexacarbonyl precursors with visible light provides information regarding thermal deposition mechanisms. By directly comparing elemental compositions of films deposited with a pulsed visible laser to those with a CW visible laser, we can determine if there are any differences between steady state and transient heating of the film surface during deposition.

Laser heating with a CW visible laser has shown that incorporation of carbon and oxygen in the growing film, under high-vacuum conditions, is a direct result of CO dissociation on the metal film surface.[20] The important reactions, determined by Houle and Singmaster for deposition of Cr, Mo and W from the corresponding hexacarbonyl, are summarized in eqs 1–4.

$$M(CO)_6(g) \rightarrow M(CO)_6(a) \quad (1)$$

$$M(CO)_6(a) \rightarrow M(a) + 6CO(a) \quad (2)$$

$$CO(a) \rightarrow CO(g) \quad (3)$$

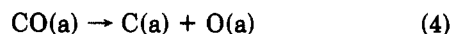

$$CO(a) \rightarrow C(a) + O(a) \quad (4)$$

Step 1 shows the adsorption of the precursor on the surface. The flux of the precursor at the surface is calculated to be 2×10^{18}, 1×10^{19}, and 3×10^{19} molecules $cm^{-2}\ s^{-1}$, for $W(CO)_6$, $Mo(CO)_6$, and $V(CO)_6$, respectively. Step 2 represents the rapid sequential decarbonylation of $M(CO)_6$ after adsorption. Steps 3 and 4 involve reactions of CO; CO can either desorb from the surface (3) or dissociate on the surface (4). The relative rates of CO desorption and dissociation were determined to be the most important factor relating to film contamination. A rigorous calculation of the surface temperature revealed that CO dissociation was important only at temperatures below 450 K.[20] Thus laser heating of the film to 450 K or higher produces clean metallic films. Using the kinetic parameters given by Houle and Singmaster, the relative rate of step 4 to step 3, i.e., $k_{dissociation}/k_{desorption}$, is calculated to be on the order of 1×10^5 at 350 K and 0.1 at 500 K.[20]

The results presented in this study show that Mo and W deposited by pulsed visible LCVD produce films which contain detectable levels of carbon and oxygen, on the order of 25% (see Tables I and II). Carbon and oxygen impurities in films deposited with a pulsed laser can arise from several sources including deposition at temperatures below 450 K which would lead to dissociation of adsorbed CO, incomplete decarbonylation of $M(CO)_6$, and readsorption of gas phase CO produced from the decarbonylation of the parent hexacarbonyl. Houle and Yeh have shown with mass spectrometry that additional reactions continue at the film surface once CW irradiation is terminated.[30] Therefore, it is highly likely that reactions occur during the laser pulse and in between pulses in pulsed LCVD. Deposition with a pulsed laser produces transient heating of the film surface and the variation in the surface temperature can also effect the deposition mechanism.

To determine the temperature at which deposition occurs, we have calculated the temperature rise at the film surface. An approximate calculation of the maximum temperature rise at the film surface can be performed with several assumptions regarding the optical and thermal properties of the growing film and the spatial and temporal profiles of the laser beam. First, we assume that the laser energy absorbed by the growing film is determined by the optical properties of the metal at 562 nm and that the dissipation of heat is determined by the thermal properties of the silicon substrate. The first assumption is, of course, false during the initial stages of film growth but is reasonable after deposition of a few hundred angstroms. Thus we will consider only growth of thick films (>300 Å) and not the more complicated initial growth period.

(30) Houle, F. A.; Yeh, L. *J. Phys. Chem.* **1992**, *96*, 2691.

The maximum temperature rise at the surface can be calculated using the equation that has been previously derived for laser-induced desorption:[31]

$$\Delta T_{max} = \tfrac{4}{3}(1 - R)[4 - t_r/t_0]^{-1/2}(2I_z/K)[\kappa t_0/\pi]^{1/2} \quad (5)$$

where R = reflectivity of the metal at 562 nm, t_r = temporal rise time, t_0 = temporal pulse width, I_z = laser intensity along the surface normal, K = thermal conductivity, κ = thermal diffusivity ($=K/\rho C$), ρ = density, and C = specific heat. In the derivation of eq 5 the laser beam temporal profile was taken to be triangular in shape, and the laser beam intensity was assumed to be uniform. The assumption of a spatially homogeneous laser beam is only roughly valid at best for the dye fundamental beam, so in the real system the temperature across the film surface will vary.

Equation 5 is valid if the thermal diffusion length, $d = (2\kappa t)^{1/2}$, is large compared to the optical penetration depth (skin depth), $d' = \lambda/4\pi k$, and if the thermal diffusion length is small compared to the radial dimensions of the beam; both of these approximations are quite reasonable for metals. In the case of pulsed LCVD of metal films on a silicon substrate when the optical properties are determined by the growing metal film[32] and the thermal properties are determined by the Si substrate, these two assumptions are also valid. It is also assumed that the thermal properties are temperature independent. While a good approximation for metals it is not valid for Si. Therefore, using the room temperature values for the thermal conductivity and heat capacity of silicon leads to a lower bound for the temperature.

With the above considerations, the maximum temperature reached at the surface of a W film is calculated to be 920 and 520 K for a laser beam energy of 166 and 60 mJ/cm^2 per pulse, respectively. This represents the upper and lower limits obtained for the range of laser energies used in these experiments. For Mo films, the maximum temperature reached at the film surface will decrease as a function of time because of window deposits. Before substantial window deposits have formed, the maximum temperature rise at the Mo film surface is calculated to be 850 and 590 K, using the initial laser beam energies of 173 and 92 mJ/cm^2 per pulse.

The calculations show that the temperature of the film surface increases above 450 K, which according to CW LCVD studies, would indicate that clean films should be produced while the laser light is incident on the sample. However, the temperature will decrease to near its initial value approximately 1 μs after the pulse.[33] As the temperature of the film decreases below 450 K, dissociation of CO begins to compete favorably with desorption, producing a layer of metal containing C and O. As a new laser pulse reaches the film surface, the temperature is again raised and desorption of CO is favored. It is possible that adsorbed carbon and oxygen produced by dissociation during the "cool" period, i.e., when the laser beam is off, could recombine and desorb during the next laser pulse, but low-coverage surface studies of CO on single-crystal Mo and W surfaces indicate that this process should not be accessible until temperatures above 1000 K are reached,[19,34-36] higher than the calculated temperatures. In addition, it has been shown that laser induced recombinatory desorption of CO is an extremely inefficient process.[37]

We can use the kinetic simulation and growth rate calculations of Houle and Singmaster[20] to determine the amount of material deposited when the laser beam is on and when it is off. We will assume that the temperature at the film surface is represented by a step function corresponding to a maximum surface temperature for 1 μs. The use of a step function will overestimate the amount of material deposited during the time the laser beam is on. Assuming a maximum temperature of 800 K, the amount of material deposited during one pulse, using the calculated growth rate of 1.7 × 10^5 Å/s at this temperature, is estimated to be 0.2 Å. To calculate the amount of material deposited when the laser beam is off the temperature at the film surface is assumed to decrease to T = 325 K for the time between pulses, 0.1 s. A temperature of 325 K is used because it is the lowest temperature for which the deposition rate was calculated.[20] If the sample does cool to near 300 K between laser pulses, this will overestimate the amount of material deposited during this time. The growth rate has been calculated to be on the order of 95 Å/s at 325 K,[20] and thus 9.5 Å will be deposited in 0.1 s. The overall average deposition rate is then calculated to be on the order of 97 Å/s.

The preceding analysis is, of course, an oversimplification of the problem, but is instructive in that it indicates most of the film is likely being deposited while the laser beam is off, this is true despite a considerably slower deposition rate compared to when the laser beam is incident on the surface and is dictated by the low duty cycle of the laser source.

Phenomenological deposition rates, calculated from sputter depth profiles and profilometer measurements, are on the order of 1 Å/s in these experiments. The phenomenological deposition rate includes both the nucleation rate and the bulk growth rate after nucleation, whereas the calculated growth rates are for the bulk growth regime only. The nucleation rate can be several orders of magnitude slower, and its contribution to the phenomenological deposition rate is probably one of the reasons for the discrepancy between the calculated value and the experimental results. Considering the simplicity of the analysis and the assumptions made, agreement between the calculated values and the experimental results can be expected to be within only 1–2 orders of magnitude.

Other sources of impurity incorporation (vide supra) included incomplete decarbonylation of the precursor and adsorption of gas phase CO produced during deposition. CW visible LCVD produces pure metal films, indicating that complete decarbonylation is achieved, and we assume that this is also the case during pulsed LCVD. Adsorption and dissociation of gas-phase CO may also contribute to the incorporation of impurities during pulsed LCVD. Deposition rates are orders of magnitude slower during pulsed LCVD, due to slower deposition rates compared to CW LCVD, which favors the adsorption of gas phase CO.

Pulsed UV LCVD of Mo and W Films. CW-UV deposition onto a room-temperature substrate is the result of photochemical reactions, both in the gas phase and on the surface when the laser is kept at moderate powers.[3] Two other mechanisms must be considered when depositions are done with a pulsed laser; multiphoton reactions

(31) Burgess, D.; Stair, P. C.; Weitz, E. *J. Vac. Sci. Technol. A* **1986**, *4*, 1362.

(32) Because of the lack of information concerning the optical properties of metal oxycarbides, the reflectivities of the pure metals are used in the temperature calculations (R = 0.50, 0.56 and 0.53 for W, Mo, and V, respectively, at 562 nm).

(33) Brand, J. L.; George, S. M. *Surf. Sci.* **1986**, *167*, 341.

(34) Ko, E. I.; Madix, R. J. *Surf. Sci.* **1981**, *109*, 221.

(35) Guillot, C.; Riwan, R.; Lecante, J. *Surf. Sci.* **1976**, *59*, 581.

(36) Benziger, J. B.; Ko, E. I.; Madix, R. J. *J. Catal.* **1978**, *54*, 414.

(37) Hall, R. B. *J. Phys. Chem.* **1987**, *91*, 1007.

and laser heating of the surface. These two pathways should result in either greater decarbonylation of the gas-phase species, through multiphoton absorption, or desorption of CO from the film surface due to laser heating. Both mechanisms, if operative, would result in a decrease in the levels of C and O incorporated in the growing film. LCVD of films deposited with a CW-UV laser, under high-vacuum conditions and exposed to air, reveal metal contents of 57% for W and 32% for Mo, after sputtering,[3] both values below those obtained in this work (see Tables I and II). Although it is somewhat difficult to make a direct comparison of the CW-UV and pulsed UV LCVD results because the experiments were done under different conditions, it is apparent that cleaner films are obtained in pulsed UV LCVD. The maximum temperature rise at the film surface is not calculated since films deposited in this manner are only a few hundred angstroms thick (200–400 Å), smaller than the optical skin depth of the metal and invalidating the assumption that the optical properties of the growing film are solely determined by the metal. A more rigorous temperature calculation, which is currently in progress, is needed in order to address whether a multiphoton or thermal mechanism is the cause of the cleaner films deposited with pulsed UV as compared to CW-UV light.

Pulsed UV and Visible LCVD of V Films from $V(CO)_6$. Determining the effects of exposure to air on the composition of vanadium films is difficult to ascertain at this time because this is the first LCVD of V thin films from $V(CO)_6$. There is a significant oxygen gradient in the first 300–400 Å of the film, indicating that the reactivity of oxygen with V films is greater than that with either Mo or W films. We can employ the assumptions made for W and Mo films regarding the effect of exposure to air in the analysis of the V films. Thus, we will assume that 562-nm bulk compositions are not affected by exposure to air, while the C/V ratio will fall somewhere between the sputtered and unsputtered value for 281-nm deposition. This places the C/V ratio for 281-nm deposition nm between 0.3 and 0.5 and the O/V ratio below 0.8. Comparison to measured standards indicates stoichiometries on the order of one vanadium atom per CO (VCO). Deposition at both wavelengths, 281 and 562 nm, results in the loss of approximately five CO groups per V atom.

The C/V ratio for films deposited at both wavelengths decreases a small amount upon sputtering, but not as much as for Mo and W films which exhibit an appreciable decrease in the C/M ratio. We conclude that metal enrichment in V films is minimal going from the surface to the bulk of the film.

The maximum temperature reached at the vanadium film surface, during laser irradiation at 562 nm, is calculated to be 520 and 800 K for laser energy densities of 67 and 145 mJ/cm^2 per pulse, respectively, the range used in our experiments. The maximum temperature at the surface decreases with time as film deposition on the pyrex window increases.

The deposition rates determined for V films are slightly higher, ~3 Å/s, than those obtained for W and Mo which may reflect the enhanced flux at the surface or the greater reactivity of $V(CO)_6$ with vanadium metal. A more complete analysis of LCVD of V from $V(CO)_6$ is difficult at this time because there is little literature data on the surface chemistry of vanadium or the reactivity of CO and $V(CO)_6$ with vanadium surfaces.

Conclusion

We have employed a 10-Hz nanosecond pulsed laser source to deposit W, Mo, and V films, from the decomposition of the corresponding hexacarbonyl, at two wavelengths, 562 and 281 nm. W and Mo films deposited with 562-nm light contain impurity levels on the order of 20–30%, significantly greater than films deposited with a CW Ar^+ laser at comparable wavelengths. Variation in film temperature during deposition due to transient heating with a pulsed laser compared to steady-state heating with a CW laser is proposed to be the cause of these differences. Films deposited with pulsed UV irradiation have a smaller level of impurities incorporated in the films as compared to CW-UV irradiation. This difference can be attributed to a thermal and/or multiphoton mechanism with the pulsed laser. Vanadium films produced via pulsed LCVD of $V(CO)_6$ under high-vacuum conditions have the same film composition at both wavelengths.

Acknowledgment. The authors would like to thank Professor Louis Messerle for providing $V(CO)_6$. We gratefully acknowledge support from the donors of the Petroleum Research Fund, administered by the American Chemical Society. S.M.S. and P.C.C. acknowledge REU support from the National Science Foundation (CHE-9000879).

Registry No. W, 7440-33-7; Mo, 7439-98-7; V, 7440-62-2.